

# The Solar *Hep* Process

*Kuniharu Kubodera*

Department of Physics and Astronomy, University of South Carolina, Columbia, SC 29208;

e-mail: kubodera@sc.edu

*Tae-Sun Park*

Schhol of Physics, Korea Institute for Advanced Study, Seoul 130-012, Korea;

e-mail: tspark@kias.re.kr

KEYWORDS: solar burning, solar neutrinos, neutrino oscillations, effective field theory

**ABSTRACT:** The *Hep* process is a weak-interaction reaction,  ${}^3\text{He} + p \rightarrow {}^4\text{He} + e^+ + \nu_e$ , which occurs in the sun. There is renewed interest in *Hep* owing to current experimental efforts to extract from the observed solar neutrino spectrum information on non-standard physics in the neutrino sector. *Hep* produces highest-energy solar neutrinos, although their flux is quite modest. This implies that the *Hep* neutrinos can at some level influence the solar neutrino spectrum near its upper end. Therefore, a precise interpretation of the observed solar neutrino spectrum requires an accurate estimate of the *Hep* rate. This is an interesting but challenging task. We describe the difficulties involved and how the recent theoretical developments in nuclear physics have enabled us to largely overcome these difficulties. A historical survey of *Hep* calculations is followed by an overview of the latest developments. We compare the results obtained in the conventional nuclear physics approach and those obtained in a newly developed effective field theory approach. We also discuss the current status of the experiments relevant

to *Hep*.

CONTENTS

INTRODUCTION . . . . . 3

EARLIER CALCULATIONS . . . . . 8

RECENT CALCULATIONS – THEORETICAL FRAMEWORK . . . . . 11

*Standard Nuclear Physics Approach (SNPA)* . . . . . 11

*Effective Field Theory (EFT)* . . . . . 13

*Nuclear EFT in the Weinberg Scheme –  $\Lambda$ -Counting* . . . . . 16

*Nuclear EFT in the KSW Scheme –  $Q$ -Counting* . . . . . 17

*Hybrid EFT* . . . . . 17

*EFT\* or MEEFT* . . . . . 18

NUMERICAL RESULTS . . . . . 19

*Hep Calculation Based on SNPA* . . . . . 19

*Hep Calculation Based on EFT\** . . . . . 19

*Off-Shell Problem* . . . . . 20

COMPARISON WITH EXPERIMENTAL DATA . . . . . 22

RELATED TOPICS . . . . . 24

*The  $pp$  Fusion Process* . . . . . 24

*Neutrino-deuteron reactions* . . . . . 25

*Hen process* . . . . . 26

SUMMARY AND OUTLOOKS . . . . . 26

## 1 INTRODUCTION

The *Hep* process,  ${}^3\text{He} + p \rightarrow {}^4\text{He} + e^+ + \nu_e$ , is one of the thermonuclear reactions that occurs in the sun. To explain why this specific process is of current interest, we first briefly describe the standard solar model, the solar neutrinos and neutrino oscillations.

The sun generates its energy by converting four protons into an alpha particle,  $4p \rightarrow {}^4\text{He} + 2e^+ + 2\nu_e$ , via chains of thermonuclear reactions caused by weak, electromagnetic, or strong interactions. The *pp*-chain, shown in Fig. 1, represents by far the most important scheme by which the  $4p \rightarrow {}^4\text{He}$  burning takes place in the sun. To establish how these reactions actually proceed in the sun, one must carry out a detailed simulation in which the radial profiles of the mass density, temperature, chemical composition, *etc.*, are determined in such a manner that hydrostatic equilibrium is satisfied and the empirically known solar properties come out correctly. The principal inputs that go into this simulation are the nuclear reaction rates, equation of state, elemental abundances, and radiative opacity. Over the past four decades a great deal of effort has been invested in this subject, and out of this endeavor has emerged a quantitative model of the sun, called the standard solar model (SSM) (1-5). Among many quantities determined by SSM are the time rates of the thermo-nuclear reactions occurring in the sun (3); Figure 1 indicates the predicted branching ratios of the various paths involved in the *pp*-chain. Among the reactions featured in Fig. 1, five are weak-interaction processes that emit solar neutrinos, and SSM predicts the flux  $\phi_\nu$  from each source of the solar neutrinos (3); this prediction is shown in Fig. 2. Studying the solar neutrinos is very important for two reasons. First, it gives direct information about the physics of the solar interior, since the neutrinos

exiting the sun experience hardly any interactions with the solar medium other than refractive effects (related to the MSW effect to be discussed later). This should be contrasted with the behavior of the photons, which interact with the solar medium so many times that, by the time they reach the surface (after  $\sim 40,000$  years !), they do not carry much information about the solar interior. Second, the solar neutrinos can provide valuable information on the properties of the neutrinos themselves; the sun is an extremely strong neutrino source and hence can be highly useful for neutrino physics.

The first measurement of the solar neutrinos was done by Davis and his collaborators (6), who used a  $^{37}\text{Cl}$  target. The results indicated that the sun indeed emits neutrinos whose flux is in approximate agreement with the SSM prediction (7), which supports the basic idea of the thermonuclear origin of the solar energy. At a more quantitative level, however, the measured flux was significantly lower than predicted by SSM. This deficit, or “solar neutrino problem”, was also confirmed by water Cerenkov counter experiments at the Kamiokande (8) and Super-Kamiokande (9), by gallium-target experiments (10, 11), and by heavy-water Cerenkov counter experiments at the Sudbury Neutrino Observatory (SNO) (12). It is to be noted that because of different detection threshold energies (see Fig. 2), these experiments are sensitive to different regions of the solar neutrino spectrum. If we denote by  $R$  the ratio of the observed event rate for a given solar neutrino detection experiment to the event rate expected from the SSM prediction, the current status of the solar neutrino problem is summarized as follows:  $R = 0.34 \pm 0.03$  for the chlorine experiment (13);  $R = 0.465 \pm 0.015$  for the water Cerenkov counter experiment (14);  $R = 0.54 \pm 0.03$  for the gallium experiments (15–17);  $R = 0.35 \pm 0.02$  (18, 19) and  $R = 0.32 \pm 0.02$  (20)

for the heavy-water Cerenkov counter experiments. It should be mentioned that the errors attached to the above values of  $R$  only include experimental errors. Obviously, the degree of seriousness of the solar neutrino problem ( $R < 1$ ) hinges on the accuracy of the SSM predictions. The latest discussion of the errors to be assigned to the SSM predictions (3) finds it extremely unlikely that the solar neutrino deficit can be attributed to the uncertainties in SSM. This conclusion is further corroborated by highly stringent constraints imposed by the helioseismological data (21).

The above discussion presupposes that the neutrinos created in the sun travel to the terrestrial detectors without changing their identity (or flavor). Let us recall that there are three distinct neutrinos, – electron neutrinos ( $\nu_e$ ), muon neutrinos ( $\nu_\mu$ ), and tau neutrinos ( $\nu_\tau$ ) — and that it is the electron neutrinos that are produced in the sun. If there exists a mechanism (22, 23) that changes electron neutrinos muon neutrinos or tau neutrinos before they reach a terrestrial detector that detects only electron neutrinos, then there would be an effective deficit of solar neutrinos. This transmutation of the neutrino flavor, called neutrino oscillations, signals physics that goes beyond the well-established standard model of particle physics, and therefore its experimental verification is of paramount importance. Neutrino oscillations can occur either during the neutrino's propagation in vacuum (22, 23), or as the neutrinos travel in matter and experience refractive interactions with the medium (MSW effect) (24).

Now, neutrinos can be detected either via charged-current (CC) reactions or via neutral-current (NC) reactions. Since a CC reaction involves the change  $\nu_x \rightarrow x$  (where  $x = e^-, \mu^-,$  or  $\tau^-$ ), it can occur only for the electron neutrino; the muon and tau-lepton are too heavy to be created by solar neutrinos. Meanwhile, an NC

reaction that involves  $\nu_x \rightarrow \nu_x$  occurs with the same amplitude for any neutrino flavor  $x$ . At SNO, the CC reaction  $\nu_e d \rightarrow e^- pp$  was used to register the electron neutrino flux  $\phi_{\nu_e}$ , whereas the NC reaction  $\nu_x d \rightarrow \nu_x np$  was used to determine the total neutrino flux,  $\phi_{\nu,T} \equiv \phi_{\nu_e} + \phi_{\nu_\mu} + \phi_{\nu_\tau}$ . The NC reaction data (18) showed that  $\phi_{\nu,T}$  agrees very well with the SSM prediction (3), whereas the CC reaction data (12) indicated  $R = 0.347 \pm 0.029$ . These results have firmly established flavor transmutations in the solar neutrinos. (For the evidence obtained from comparison of the SNO CC reaction data and the Super-Kamiokande data (14), see Reference (12).) Independent evidence for neutrino oscillations is known from the study of the atmospheric neutrinos at Super-Kamiokande (25), and from the study of the reactor neutrinos at the KamLAND (26).

Neutrino oscillations occur if a neutrino state produced in a weak-interaction process (“weak eigenstate”) is different from an eigenstate of the Hamiltonian (mass eigenstate), and if the mass eigenstates of different neutrinos are not degenerate. It is conventional to parametrize the former aspect in terms of mixing parameters, and the latter in terms of differences between the neutrino masses squared ( $\delta m^2$ 's). Now that the existence of neutrino oscillations has been established, the next important challenge is to determine the accurate values of the mixing parameters and  $\delta m^2$ 's, quantities that should carry valuable information on new physics beyond the standard model. (For a recent survey of this topic, see *e.g.*, Reference (27).) The great importance of this determination makes it highly desirable to assemble an over-constraining body of data, and this is one reason why detailed studies of the solar *Hep* process can be important.

In discussing *Hep*, it is convenient to use Bahcall *et al.*'s latest treatise on the SSM (3) as a basic reference (to be called BP00). According to BP00, the

neutrino flux due to *Hep* is  $\phi_\nu(\text{hep}) = 9.4 \times 10^3 \text{ cm}^{-2}\text{s}^{-1}$ , which is seven orders of magnitude smaller than the *pp*-fusion neutrino flux, and three orders of magnitude smaller than the  $^8\text{B}$  neutrino flux  $\phi_\nu(^8\text{B})$ ; the smallness of  $\phi_\nu(\text{hep})$  can also be seen from Fig. 2. (For the radial distribution of sites of *Hep* neutrino generation inside the sun, see Fig. 6.1 in Reference (2).) Because of its extremely small branching ratio (see Fig. 1), *Hep* in fact does not affect solar model calculations. So why does it interest us? One reason is that *Hep* is a potential source of useful information on non-standard physics in the neutrino sector. *Hep* generates neutrinos having maximum energy  $E_\nu^{\text{max}}(\text{hep}) = 18.8 \text{ MeV}$ , which is higher than that of the  $^8\text{B}$  neutrinos,  $E_\nu^{\text{max}}(^8\text{B}) = 17 \text{ MeV}$ ; thus the *Hep* neutrinos near the upper end of their spectrum represent the highest-energy solar neutrinos (see Fig. 2). Solar neutrino detectors such as Super-Kamiokande and SNO can determine the spectrum of the solar neutrinos in a region dominated by the  $^8\text{B}$  neutrinos. Meanwhile, the shape of  $\phi_\nu(^8\text{B})$  is independent of solar models to an accuracy of 1 part in  $10^5$  (28). Therefore, in the absence of *Hep* neutrinos, any deviation of the observed  $\phi_\nu$  from  $\phi_\nu(^8\text{B})$  in the higher  $E_\nu$  region reflects the non-standard behavior of neutrinos. Solar neutrino experiments that approach the level of precision needed for studying this deviation have already been reported from Super-Kamiokande (14, 29, 30) (see below). Apart from the ramifications for neutrino physics, the study of *Hep* neutrinos is also important as a possible additional check of the SSM itself.

In interpreting these and future experiments, we need to know accurately to what extent the *Hep* neutrinos can affect  $\phi_\nu$  in the  $^8\text{B}$  neutrino region (1, 31–33), and for this we must make a reliable estimation of the *Hep* cross section. This task, however, turns out to be extremely challenging. For one thing, although the

primary  $Hep$  amplitude is formally of the Gamow-Teller (GT) type, the usually dominant one-body GT amplitude is strongly suppressed for  $Hep$  (see below). Furthermore, the two-body corrections to the “leading” one-body GT term have opposite sign, causing a large cancellation. It is therefore necessary to calculate these “corrections” with great accuracy, which is a highly non-trivial task. Thus, from a nuclear-physics point of view,  $Hep$  presents a difficult yet very intriguing challenge.

In what follows, we first present a history of  $Hep$  calculations, explaining in more detail the nature of the difficulties involved in  $Hep$  calculations. We then describe how the recent theoretical developments in nuclear physics have enabled us to largely overcome these difficulties. After reporting the latest results obtained in the so-called standard nuclear physics approach, we highlight the results obtained in a newly developed effective field theory approach. We then describe the current status of experimental information on the  $Hep$  neutrinos. At the end we discuss several electroweak processes closely related to the  $Hep$  calculations.

## 2 EARLIER CALCULATIONS

An illuminating survey of the earlier  $Hep$  calculations can be found in References (33, 34). The  $Hep$  reaction rate can be conveniently expressed in terms of the astrophysical  $S$ -factor defined by  $S(E) = E\sigma(E)\exp(4\pi\alpha/v_{\text{rel}})$ , where  $\sigma(E)$  is the  $Hep$  cross section at center-of-mass energy  $E$ ,  $v_{\text{rel}}$  is the relative velocity between  $p$  and  ${}^3\text{He}$ , and  $\alpha$  is the fine structure constant;  $S(E)$  is a smooth function of  $E$  that remains non-vanishing as  $E \rightarrow 0$ . The first  $Hep$  calculation in 1952 by Salpeter (35) was based on the extreme single-particle picture and only considered the overlap between an  $s$ -wave proton scattering wave function and



a  $1s$  neutron state in  ${}^4\text{He}$ . This simplified treatment led to a large value for  $S$ ,  $S(0) = 630 \times 10^{-20}$  keV-b, and this value was used by Kuzmin (31), who was the first to discuss *Hep* in connection with solar neutrinos. Werntz and Brennan (36) pointed out the drastic suppression of the *Hep* rate due to a specific feature of the initial and final nuclear wave functions. The dominant component of  ${}^4\text{He}$  has the orbital configuration  $(1s)^4$ , which is totally symmetric, *i.e.*, a state with  $[4]$  orbital permutation symmetry. In general, the Pauli principle dictates that a spin-isospin wave function accompanying an orbital function with  $[4]$  symmetry must be totally antisymmetric ( $[1111]$  state) and hence must have  $S = T = 0$ . The contraposition of this property implies that the  $p$ - ${}^3\text{He}$  state with isospin  $T = 1$  cannot have  $[4]$  orbital symmetry. Meanwhile, the one-body GT operator,  $\sum_{i=1}^4 \boldsymbol{\sigma}(i)\tau_-(i)$ , acting only on the spin and isospin, cannot change the symmetry properties of orbital wave functions. For *Hep*, therefore, the leading one-body GT operator cannot connect the main components of the initial and final states — a feature that leads to a drastic suppression of the *Hep* amplitude. This implies that the exchange-current (EXC) effects may play an exceptionally large role here. Werntz and Brennan (36) attempted to relate the *Hep* rate to the M1 matrix element for the *Hen* process, where *Hen* is radiative capture of a thermal neutron on  ${}^3\text{He}$ :  ${}^3\text{He} + n \rightarrow {}^4\text{He} + \gamma$ . They assumed (a) the validity of isospin symmetry apart from the difference in the radial functions of the incident nucleons (proton for *Hep* and neutron for *Hen*); and (b) that two-body EXC terms dominated for both *Hep* and *Hen* and that their matrix elements could be related to each other via an isospin rotation. Based on the upper limit for the *Hen* cross section known at that time, Werntz and Brennan gave an upper limit for the *Hep*  $S$ -factor,  $3.7 \times 10^{-20}$  keV-b, which was about 200 times smaller than Salpeter's estimate. Later

Wernitz and Brennan (37) refined their estimate in several respects, including the addition of the contributions from  $p$ -wave capture channels, and they arrived at an  $S$ -factor of  $8.1 \times 10^{-20}$  keV-b. Tegnér and Bargholtz (38) also attempted to relate  $Hep$  to  $Hen$ , but they pointed out the importance of the contributions due to the  $D$ -state components in the  ${}^3\text{He}$  and  ${}^4\text{He}$  wave functions, and they used the EXC operators of the type derived by Chemtob and Rho (39); Tegnér and Bargholtz's estimate was  $(4 - 25) \times 10^{-20}$  keV-b, where the spread corresponded to the range of the experimental values of the  $Hen$  cross section before 1983. This result was sharpened by Wolfs *et al.* (40), who measured the  $Hen$  cross section precisely and reported a value of  $(54 \pm 6) \times 10^{-20}$   $\mu\text{b}$ ; their estimate of the  $Hep$   $S$ -factor was  $(15.3 \pm 4.7) \times 10^{-20}$  keV-b. Wervelman *et al.* (41) also made a precision measurement of the  $Hen$  cross section and obtained  $(55 \pm 3) \times 10^{-20}$   $\mu\text{b}$ , in good agreement with that obtained by Wolfs *et al.*. However, Wervelmann *et al.* predicted a  $Hep$   $S$ -factor of  $(57 \pm 8) \times 10^{-20}$  keV-b. These estimates should be considered semi-quantitative, since even the estimates of the one-body terms differ wildly from model to model, and furthermore it is known (39) that the EXC for GT transitions should differ from that for M1 transitions. Subsequently, Carlson *et al.* (42) showed that there is a significant cancellation between the one-body and two-body terms and that the use of realistic wave functions (as opposed to schematic wave functions employed in the previous calculations) is crucial for a reliable estimation of the  $Hep$  rate. These authors performed a variational Monte Carlo calculation and, with the use of EXC operators derived from pion- and  $\rho$ -exchange diagrams and  $\Delta$ -excitation diagrams, they obtained  $S = 1.3 \times 10^{-20}$  keV-b (42). Schiavilla *et al.* (43) performed a similar calculation but with the use of explicit  $\Delta$  degree of freedom and obtained  $S = (1.4 - 3.2) \times 10^{-20}$  keV-b.

The *Hep* calculations up to this point only considered the contribution of the *s*-wave capture channel, except in the work of Werntz and Brennan (37). Horowitz (44) presented a new estimate of the contribution of the *p*-wave capture channel, using schematic wave functions, and emphasized that it could be of substantial magnitude. We categorize *Hep* estimations that have appeared since 2000 as “recent” calculations and discuss them in the next section.

As the above survey shows, the calculated value of the *Hep* *S*-factor changed by two orders of magnitude from the original Salpeter value. Fortunately, however, an encouraging sign of convergence in the *Hep* *S*-factor has been emerging over the past few years. This is attributable, first, to further significant progress along the line of work following References (42,43). Second, the application of effective field theory to *Hep* has greatly increased the reliability of the calculated *S*-factor. These latest developments are the subjects of the following sections. To present them coherently, we first survey the relevant theoretical frameworks in a somewhat general context, and then proceed to discuss the specific numerical results for *Hep*.

### 3 RECENT CALCULATIONS – THEORETICAL FRAMEWORK

#### 3.1 Standard Nuclear Physics Approach (SNPA)

The phenomenological potential picture has been highly successful in describing a great variety of nuclear phenomena. In this picture a model Hamiltonian for an *A*-nucleon system involves a phenomenological two-body potential  $v^{phen}$  (and, if needed, an additional phenomenological three-body potential). Once this model Hamiltonian is specified, the nuclear wave function is obtained by solving the *A*-body Schrödinger equation. Recent progress in numerical techniques for this

type of calculation has reached such a level (45) that the wave functions of low-lying levels for light nuclei can now be obtained nearly without approximation. This achievement frees us from the “usual” nuclear physics complications that arise from truncation of nuclear Hilbert space down to certain model space (such as shell-model configurations, cluster-model trial functions, *etc.*). Because there is large freedom in choosing a possible form for the short-range part of  $v^{phen}$ , one assumes a certain functional form and fixes the parameters appearing in it by demanding that the nucleon-nucleon (NN) scattering data and the deuteron properties be reproduced. There are by now several so-called high-precision phenomenological potentials that can reproduce all the existing two-nucleon data with normalized  $\chi^2$  values close to unity. In normal circumstances, nuclear responses to external electroweak probes are given, to good approximation, by one-body terms; these are also called the impulse approximation terms. To obtain higher accuracy, however, one must also consider exchange current (EXC) terms, which represent the contributions of nuclear responses involving two or more nucleons. In particular, if for some reason the impulse approximation contributions are suppressed, it becomes essential to take account of the EXC contributions. These EXC’s are usually derived from one-boson exchange diagrams, which impose the low-energy theorems and current algebra properties on the vertices featured in the diagrams (39, 46, 47). A formalism based on this picture is referred to as the standard nuclear physics approach (SNPA), also called the potential model in the literature. SNPA has been used extensively to describe nuclear electroweak processes in light nuclei, and the generally good agreement between theory and experiment (45) gives a strong indication that SNPA captures much of the physics involved. The calculations quoted earlier (42, 43) represent

the early stage of SNPA.

### 3.2 *Effective Field Theory (EFT)*

Although SNPA has been scoring undeniable successes in correlating and explaining a vast variety of data, it is still important from a fundamental point of view to raise the following issues. First, since hadronic systems are governed by quantum chromodynamics (QCD), one should ultimately be able to relate nuclear phenomena to QCD, but this relation is not visible in SNPA. In particular, whereas chiral symmetry is known to be a fundamental symmetry of QCD, SNPA is largely disjoint from this symmetry. Second, in SNPA, even for describing low-energy phenomena, we start with a “realistic” phenomenological potential that is tailored to encode short-range (high-momentum) and long-range (low-momentum) physics simultaneously. This mixing of the two different scales seems theoretically unsatisfactory. Third, in writing down a phenomenological Lagrangian for describing the nuclear interaction and nuclear responses to the electroweak currents, we find no clear guiding principle in SNPA — no obviously identifiable expansion parameter that helps us to control the possible forms of terms in the Lagrangian and that provides a general measure of errors in our calculation. To address these and related issues, a new approach based on EFT was proposed (48), and it has been studied with great intensity (for reviews, see References (49)-(50)).

The intuitive picture of EFT is rather simple. In describing phenomena characterized by a typical energy-momentum scale  $Q$ , we expect that we need not include in our Lagrangian those degrees of freedom that pertain to energy-momentum scales much higher than  $Q$ . This expectation motivates us to intro-

duce a cut-off scale  $\Lambda$  that is sufficiently large compared with  $Q$  and to classify our fields (to be generically represented by  $\Phi$ ) into two groups: high-frequency fields ( $\Phi_{high}$ ) and low-frequency fields ( $\Phi_{low}$ ). By eliminating (or “integrating out”)  $\Phi_{high}$ , we arrive at an *effective* Lagrangian that only involves  $\Phi_{low}$  as explicit dynamical variables. Using the notion of path integrals, we find that the effective Lagrangian  $\mathcal{L}_{eff}$  is related to the original Lagrangian  $\mathcal{L}$  as

$$\begin{aligned} \int [d\Phi] e^{i \int d^4x \mathcal{L}[\Phi]} &= \int [d\Phi_{high}] [d\Phi_{low}] e^{i \int d^4x \mathcal{L}[\Phi_{high}, \Phi_{low}]} \\ &\equiv \int [d\Phi_{low}] e^{i \int d^4x \mathcal{L}_{eff}[\Phi_{low}]}. \end{aligned} \quad (1)$$

One can show that  $\mathcal{L}_{eff}$  defined by eq.(1) inherits the symmetries (and the patterns of symmetry breaking, if there are any) of  $\mathcal{L}$ . It also follows that  $\mathcal{L}_{eff}$  should be the sum of all possible monomials of  $\Phi_{low}$  and their derivatives that are consistent with the symmetry requirements dictated by  $\mathcal{L}$ . Because a term that involves  $n$  derivatives scales like  $(Q/\Lambda)^n$ , the terms in  $\mathcal{L}_{eff}$  can be organized into a perturbative series in which  $Q/\Lambda$  serves as an expansion parameter. The coefficients of terms in this expansion scheme are called the low-energy constants (LECs). Insofar as all the LEC’s up to a specified order  $n$  can be fixed either from theory or from fitting to the experimental values of the relevant observables,  $\mathcal{L}_{eff}$  serves as a complete (and hence model-independent) Lagrangian to the given order of expansion.

When EFT is applied to nuclear physics, the underlying Lagrangian is the QCD Lagrangian  $\mathcal{L}_{QCD}$ , whereas, for the typical nuclear physics energy-momentum scale  $Q \ll \Lambda_\chi \sim 1$  GeV, the effective degrees of freedom that would feature in the effective Lagrangian  $\mathcal{L}_{eff}$  are hadrons rather than the quarks and gluons. It is not obvious how to apply the formal definition, eq.(1), to establish a relation between  $\mathcal{L}_{QCD}$  and  $\mathcal{L}_{eff}$  written in terms of the hadrons, since the hadrons cannot

be simply identified with the low-frequency field,  $\Phi_{low}$ , in the original Lagrangian. At present, the best one can do is to resort to symmetry considerations and the above-mentioned expansion scheme. Here chiral symmetry plays an important role. It is known that chiral symmetry is spontaneously broken, generating the pions as Nambu-Goldstone bosons. This feature can be incorporated by assigning suitable chiral transformation properties to the Goldstone bosons and writing down all possible chiral-invariant terms up to a specified chiral order (see *e.g.* Reference (51)). The above consideration presupposes exact chiral symmetry in  $\mathcal{L}_{\text{QCD}}$ . In reality,  $\mathcal{L}_{\text{QCD}}$  contains small but finite quark mass terms, which explicitly violate chiral symmetry and lead to a non-vanishing value of the pion mass  $m_\pi$ . Again, there is a well-defined method to determine what terms are needed in the Goldstone boson sector to represent the effect of explicit chiral symmetry breaking (51). We can then establish a counting rule, called chiral counting, which allows us to classify the relative importance of a term in  $\mathcal{L}_{\text{eff}}$  and a given Feynman diagram according to the number of powers in  $Q/\Lambda$  and  $m_\pi/\Lambda$ . These considerations lead to an EFT called chiral perturbation theory ( $\chi$ PT) (52, 53).

The successes of  $\chi$ PT in the meson sector are well known (see, *e.g.*, Reference (49)). A problem we encounter in extending  $\chi$ PT to the nucleon sector is that, because the nucleon mass  $m_N$  is comparable to the cut-off scale  $\Lambda_\chi$ , a simple application of expansion in  $Q/\Lambda$  does not work. This problem can be circumvented by employing heavy-baryon chiral perturbation theory (HB $\chi$ PT) (54). HB $\chi$ PT has been applied with great success to the one-nucleon sector (see *e.g.* Reference (49)). HB $\chi$ PT, however, cannot be applied in a straightforward manner to nuclear systems, because nuclei involve very low-lying excited states, and the

existence of this small energy scale spoils the original counting rule (48).

### 3.3 Nuclear EFT in the Weinberg Scheme – $\Lambda$ -Counting

Weinberg proposed to avoid this difficulty by classifying Feynman diagrams into two groups, irreducible and reducible diagrams (48). Irreducible diagrams are those in which every intermediate state has at least one meson in flight; all others are classified as reducible diagrams. We then apply the above-mentioned chiral counting rules only to irreducible diagrams. The contribution of all the two-body irreducible diagrams (up to a specified chiral order) is treated as an effective potential acting on nuclear wave functions. Meanwhile, the contributions of reducible diagrams can be incorporated by solving the Schrödinger equation. This two-step procedure may be referred to as nuclear  $\chi$ PT or, to be more specific, nuclear  $\chi$ PT in the Weinberg scheme.

To apply nuclear  $\chi$ PT to a process that involves (an) external current(s), we derive a nuclear transition operator  $\mathcal{T}$  by evaluating the complete set of irreducible diagrams (up to a given chiral order  $\nu$ ) that involve the relevant external current(s). For consistency in chiral counting, the nuclear matrix element of  $\mathcal{T}$  must be calculated with the use of nuclear wave functions that are governed by nuclear interactions that represent all the irreducible  $A$ -nucleon diagrams up to  $\nu$ -th order. If this program could be carried out exactly, it would constitute an *ab initio* calculation. The unambiguous classification of transition operators according to their chiral orders is a great advantage of EFT, which is missing in SNPA.



### 3.4 Nuclear EFT in the KSW Scheme – *Q*-Counting

An alternative form of nuclear EFT is based on the power divergence subtraction (PDS) scheme. The PDS scheme proposed by Kaplan, Savage and Wise (KSW) in their seminal papers (55) uses a counting scheme (often called *Q*-counting) that differs from the Weinberg scheme. Although a great number of important investigations have used the PDS scheme (for a review, see *e.g.* Reference (56)), here we are primarily concerned with the Weinberg scheme. The reason is that the PDS scheme has so far been used chiefly only for the two-nucleon systems (see, however, References (57–59)), and so at present it is less directly connected with the *Hep* process than the Weinberg scheme is; no *Hep* calculations based on the PDS scheme exist in the literature at the time of this writing.

### 3.5 Hybrid EFT

The preceding subsections emphasize the formal merits of nuclear EFT. In actual calculations, however, it is still a major challenge to generate, strictly within the EFT framework, nuclear wave functions whose accuracy is comparable to that of SNPA wave functions (see section 7, however). A pragmatic solution to this problem is to use wave functions obtained in SNPA; we refer to this eclectic approach as hybrid EFT (60–62). Since the *NN* interactions that generate SNPA wave functions accurately reproduce the two-nucleon data, the use of hybrid-EFT is almost equivalent to using the empirical data themselves to control the initial and final nuclear wave functions, insofar as the off-shell problem (see below) and the contributions of three-body (and higher-body) interactions are properly addressed.

### 3.6 *EFT\* or MEEFT*

Hybrid EFT can be used for light complex nuclei ( $A = 3, 4, \dots$ ) with essentially the same accuracy and ease as for the  $A=2$  system. We should emphasize in this connection that, in  $A$ -nucleon systems ( $A \geq 3$ ), the contributions of transition operators involving three or more nucleons are intrinsically suppressed according to chiral counting, and hence, up to a certain chiral order, a transition operator in an  $A$ -nucleon system consists of the same EFT-based one-body and two-body terms that are used for the two-nucleon system.

As mentioned above, the chiral Lagrangian is definite only when the values of all the relevant LECs are fixed, but there may be cases where this condition cannot be readily met. Suppose that a two-body EXC operator under consideration contains an LEC (call it  $\kappa$ ) that cannot be determined with the use of  $A=2$  data alone. It is possible that an observable (call it  $\Omega$ ) in a  $A$ -body system ( $A \geq 3$ ) is sensitive to  $\kappa$  and that the experimental value of  $\Omega$  is known with sufficient accuracy. Then we can determine  $\kappa$  by calculating the hybrid-EFT matrix element that corresponds to  $\Omega$  and adjusting  $\kappa$  to reproduce the empirical value of  $\Omega$ . Once  $\kappa$  is fixed this way, we can make predictions for any other observables for any other nuclear systems that are controlled by the same transition operators. Hybrid EFT used in this manner is referred to as EFT\* or as MEEFT (more effective EFT).

The effective Lagrangian  $\mathcal{L}_{eff}$  is, by construction, valid only below the specified cutoff scale  $\Lambda$ . This basic constraint should be respected in nuclear EFT calculations as well. One way to implement this constraint is to introduce a momentum-cutoff  $\Lambda$  for the two-nucleon relative momentum. The sensitivity of the results on the choice of  $\Lambda$  is expected to serve as a measure of uncertainties

in the calculational framework.

## 4 NUMERICAL RESULTS

### 4.1 *Hep* Calculation Based on SNPA

Marcucci *et al.* have recently carried out a highly elaborate SNPA calculation of the *Hep* rate (34,63). The treatment of the four-body wave functions was improved with the use of the correlated-hyperspherical-harmonics method (64). The strength of the dominant EXC contribution due to a  $\Delta$ -excitation diagram was adjusted to reproduce the experimental value of  $\Gamma_{\beta}^{\text{tritium}}$ , the tritium beta-decay rate:  $\Gamma_{\beta}^{\text{tritium}}(\text{exp}) = 12.32 \pm 0.03 \text{ yr}^{-1}$  (65). This type of empirical normalization, first introduced in Reference (42), is expected to reduce significantly the model dependence of the calculated *Hep* rate. Furthermore, the contribution of the initial *p*-wave channel was included. The resulting *Hep* *S*-factor at 10 keV (close to the Gamow peak) is  $S = (10.1 \pm 0.6) \times 10^{-20} \text{ keV-b}$ ; this is the value used by Bahcall *et al.* (BP00) (3). The corresponding threshold value is  $S = 9.64 \times 10^{-20} \text{ keV-b}$ .

### 4.2 *Hep* Calculation Based on EFT\*

Park *et al.* (66,67) carried out an EFT\* calculation of the *Hep* rate up to next-to-next-to-next-to-leading order in chiral counting. To this order, there appears in two-body terms one LEC that at present cannot be determined from data belonging to the  $A=2$  systems. This unknown LEC, denoted by  $\hat{d}_R$  in Reference (62), parametrizes the strength of a contact-type four-nucleon axial-current coupling. Park *et al.* noted that  $\hat{d}_R$  also appears as the only unknown parameter in the calculation of  $\Gamma_{\beta}^{\text{tritium}}$ . They determined  $\hat{d}_R$  from the experimental value

of  $\Gamma_{\beta}^{\text{tritium}}$ (65). With the value of  $\hat{d}_R$  determined this way, Park *et al.* made a parameter-free EFT\* calculation of the *Hep* rate (66, 67). The result for the threshold *S*-factor is  $S = (8.6 \pm 1.3) \times 10^{-20}$  keV-b, where the error spans the range of the  $\Lambda$  dependence. This EFT\* result supports the SNPA results in References (34, 63). It is reasonable to expect that, if the effects of neglected higher-order terms and deviations from the framework of EFT\* itself are sizable, they would cause the significant  $\Lambda$  dependence in the calculated *S*. This consideration led Park *et al.* (66, 67) to adopt the  $\Lambda$  dependence ( $\sim 15$  % variation) of  $S_{Hep}$  as a measure of uncertainties in their EFT\* calculation of  $S_{Hep}$ . The above-mentioned large cancellation between the one-body and two-body contributions in *Hep* amplifies the  $\Lambda$  dependence of  $S_{Hep}$  up to  $\sim 15$  %, but this dependence is still reasonably small. (Below we discuss the *pp*-fusion reaction, where there is no such cancellation and the  $\Lambda$  dependence is found to be extremely small.) In Fig.2, the 15 % errors assigned to  $\phi_{\nu}(hep)$  reflects the uncertainty in the EFT\* estimation of  $S_{Hep}$  in References (66, 67); this is the first time that  $\phi_{\nu}(hep)$  is presented with an error estimate attached.

### 4.3 Off-Shell Problem

The use of hybrid EFT may bring in a certain degree of model dependence due to off-shell effects, because the phenomenological *NN* interactions are constrained only by the on-shell two-nucleon observables. This off-shell effect, however, is expected to be small for the reactions under consideration, since they involve low momentum transfers and hence are not extremely sensitive to the short-range behavior of the nuclear wave functions. One way to quantify this expectation is to compare a two-nucleon relative wave function generated by the phenomeno-

logical potential with that generated by an EFT-motivated potential. Phillips and Cohen (68) made such a comparison in their analysis of the one-body operators responsible for electron-deuteron Compton scattering. They showed that a hybrid EFT should work well up to momentum transfer 700 MeV. A similar conclusion is expected to hold for a two-body operator, so long as its radial behavior is duly “smeared-out” reflecting a finite momentum cutoff. Thus, EFT\* as applied to low energy phenomena is expected to be practically free from the off-shell ambiguities.

Another indication of the stability of the EFT\* results comes from the recently developed idea of the “low-momentum nuclear potential”. Let us recall that a “realistic phenomenological” potential  $v^{phen}$  is determined by fitting to the two-nucleon data up to the pion production threshold energy. So, physically,  $v^{phen}$  should reside in a momentum regime below a certain cutoff  $\Lambda_c$ . In the conventional treatment, however, the existence of this cutoff scale is ignored. Bogner *et al.* (69) proposed to construct an “effective low-momentum” potential,  $V_{low-k}$ , by integrating out from  $v^{phen}$  the momentum components higher than  $\Lambda_c$ . They calculated  $V_{low-k}$ s corresponding to a number of well-established  $NN$  potentials. Remarkably, the resulting  $V_{low-k}$ s were found to lead to identical half-off-shell  $T$ -matrices for all the cases studied, even though the ways short-range physics is encoded in these  $v^{phen}$ s are quite diverse. This implies that the  $V_{low-k}$ s are free from the off-shell ambiguities, and therefore the use of  $V_{low-k}$ s is essentially equivalent to employing an EFT-based  $NN$  potential. The fact that EFT\* calculations by design contain a momentum-cutoff regulator essentially ensures that an electroweak transition matrix element calculated in EFT\* is only sensitive to those half-off-shell  $T$ -matrices that are controlled by  $V_{low-k}$ , and

therefore the EFT\* results reported by Park et al. (67) are expected to be essentially free from the off-shell ambiguities.

Furthermore, because correlating the observables in neighboring nuclei (as was done here) is likely to serve as an additional renormalization, the possible effects of higher-chiral-order terms and/or off-shell ambiguities can be significantly suppressed by the use of EFT\*

## 5 COMPARISON WITH EXPERIMENTAL DATA

In Super-Kamiokande experiments, information on the solar neutrino spectrum  $\phi_\nu$  was obtained by detecting the recoil electron in the reaction,  $\nu + e^- \rightarrow \nu + e^-$ , for  $E_{\text{recoil}} \geq 6.5$  MeV (29), and for  $E_{\text{recoil}} \geq 5$  MeV (14). As mentioned,  $\phi_\nu$  in this range is governed by the  $^8\text{B}$  neutrinos mixed with a tiny number of *hep* neutrinos. Reference (29) presents the data in 15 bins between 6.5 MeV and 14 MeV and one higher-energy bin covering 14 - 20 MeV. The three highest bins showed a larger number of events than expected from the then most popular neutrino oscillation parameters. Bahcall and Krastev (33) analyzed these data in detail; they considered various neutrino oscillation scenarios and treated the *Hep*  $S$ -factor,  $S_{Hep}$ , as an adjustable parameter. The philosophy behind this treatment was that, although the “1998 standard value” of  $S_{Hep}$  adopted in (70) came from an elaborate SNPA calculation (43), a first-principle physics argument was still needed to exclude the possibility that  $S_{Hep}$  might exceed, e.g., 10 times this value. Introducing the enhancement factor  $\alpha$  defined by  $\alpha \equiv S_{Hep}/(2.3 \times 10^{-20} \text{ keV-b})$ , where the denominator is the central value of the 1998 standard  $S_{Hep}$ , Bahcall and Krastev reported that, by allowing  $\alpha$  to be larger than 20, one could significantly improve global fits to all the then available solar neutrino data for every neutrino

oscillation scenario studied. This result triggered renewed theoretical efforts by Marcucci *et al.* (34, 63) and Park *et al.* (66, 67) to determine  $S_{Hep}$  with higher accuracy. An improved SNPA calculation by Marcucci *et al.* (34, 63) gave a value of  $S_{Hep}$  4.4 times larger than the “1998 standard value”; the value of  $\phi_\nu(hep)^{SSM}$  that appears in BP00 (3) is based on Marcucci *et al.*'s  $S_{Hep}$ . It is to be noted that the authors of (3) avoided giving an estimate of total uncertainty in  $\phi_\nu(hep)^{SSM}$ , citing the unique subtlety involved in the calculation of  $S_{Hep}$ .

According to the more recent Super-Kamiokande results (14) covering  $E_{recoil} \geq 5$  MeV, the observed shape of  $\phi_\nu$  is consistent with an undistorted  ${}^8\text{B}$  neutrino spectrum shape; a  $\chi^2$  fit of the overall spectrum shape resulted in  $\chi^2/\text{d.o.f.} = 19.1/18$ , without any *Hep* neutrino admixture. This is not very surprising since  $\phi_\nu(hep)$  is typically three orders of magnitude smaller than  $\phi_\nu({}^8\text{B})$ . Meanwhile, by assuming that  $1.3 \pm 2.0$  events registered in the recoil electron energy bin,  $E_{recoil} = 18 - 21$  MeV, are due to the *Hep* neutrinos, the 90 % confidence level upper limit of  $\phi_\nu(hep)$  was determined to be  $40 \times 10^3 \text{cm}^{-2}\text{s}^{-1}$  (14). This upper limit is 4.3 times the BP00 prediction for the no neutrino-oscillation assumption; thus the experimental  $\phi_\nu(hep)$  is consistent with the theoretical value. However, BP00 stressed that the significance of this agreement is limited because one cannot assign an estimate of uncertainty to the theoretical value of  $S_{Hep}$  used in BP00.

This drawback can be greatly mitigated with the use of the EFT\* calculation of  $S_{Hep}$  by Park *et al.* (66, 67), which gives  $S_{Hep}$  with a well-controlled error estimate (in the sense explained earlier). The use of the central value of  $S_{Hep}$  obtained by Park *et al.* (67) would slightly lower  $\phi_\nu(hep)^{SSM}$  but would keep its upper end compatible with  $\phi_\nu(hep)^{SSM}$  in BP00 (3). Thus, the statement that

the upper limit of the experimental  $\phi_\nu(\text{hep})$  is  $\sim 4$  times the central value of the SSM prediction remains valid. However, with the use of  $S_{\text{Hep}}$  obtained in the EFT\* calculation, the SSM prediction is controlled within  $\sim 15\%$  precision, and this fact is expected to be valuable in future analyses of experiments concerning *Hep* neutrinos. Corradu et al. (71) pointed out that, with the precision of  $S_{\text{hep}}$  achieved in Reference (67), we may be able to use the  $\phi_\nu(\text{hep})$  data to study the possible nonstandard behavior of the solar core plasma.

## 6 RELATED TOPICS

We have so far concentrated on the calculations of *Hep*. To further clarify the key aspects involved in these calculations, we now discuss the related problems of evaluating the cross sections for the *pp* fusion reaction ( $p + p \rightarrow d + e^+ + \nu_e$ ), the neutrino-deuteron reactions, and the *Hen* reaction.

### 6.1 The *pp* Fusion Process

The latest SNPA estimation of the *pp* fusion rate was carried out by Schiavilla *et al.* (72), using the EXC operator whose strength was normalized to fit  $\Gamma_\beta^{\text{tritium}}$ . Park *et al.* (67, 73) performed an EFT\* calculation of the *pp* fusion rate, using exactly the same method employed for the *Hep* calculation. The result is  $S_{pp} = 3.94 \times (1 \pm 0.005) \times 10^{-25}$  MeV b. This EFT\* result supports the value of  $S_{pp}$  obtained in SNPA (72). It has been found that  $S_{pp}$  in the EFT\* calculation varies by only  $\sim 0.1\%$  against changes in  $\Lambda$ , and this feature can be regarded as typical for unsuppressed transitions such as *pp* fusion. Thus, to the extent that the  $\Lambda$  dependence serves as a reasonable measure of theoretical uncertainties (as discussed above), the EFT\* prediction of  $S_{pp}$  can be considered highly



robust. The 0.5 % error in the above  $S_{pp}$  is dominated by the uncertainty in the experimental value of  $\Gamma_{\beta}^{\text{tritium}}$ .

The PDS scheme also was used to estimate the  $pp$  fusion rate (74). Taking advantage of very low energy and momentum involved in this reaction, Kong and Ravendal used “nucleon-only” EFT (without pions). To the order they considered, there appears only a single LEC, denoted by  $L_{1A}$ , and there have been attempts to constrain its value using observables in the two-nucleon systems (75).

## 6.2 Neutrino-deuteron reactions

The  $\nu$ - $d$  cross sections for  $E_{\nu} \lesssim 20$  MeV are very important in connection with the SNO experiments. Nakamura *et al.* performed a detailed SNPA calculation of the  $\nu$ - $d$  cross sections  $\sigma(\nu d)$  (76,77), and Butler *et al.* (78) carried out an EFT calculation of  $\sigma(\nu d)$ , using the PDS scheme (55). The EFT results (78) agree with the SNPA results (77), if the above-mentioned unknown LEC,  $L_{1A}$ , involved in the PDS scheme is suitably adjusted. The optimal value,  $L_{1A} = 5.6 \text{ fm}^3$ , found by Butler *et al.* (78) is consistent with the order of magnitude of  $L_{1A}$  expected from the naturalness argument (based on a dimensional analysis),  $|L_{1A}| \leq 6 \text{ fm}^3$ . Even though it is reassuring that  $\sigma(\nu d)$  calculated in SNPA and EFT agree with each other (in the above-explained sense), it is desirable to carry out an EFT calculation that is free from any adjustable LEC. EFT\* allows us to carry out an EFT-controlled parameter-free calculation of  $\sigma(\nu d)$ , and Ando *et al.* (79) performed such a calculation. The  $\sigma(\nu d)$ s they obtained (79) are found to agree within 1% with  $\sigma(\nu d)$ 's obtained in SNPA (77). Although it is in principle possible to calculate the tritium beta decay rate in the PDS scheme and use  $\Gamma_{\beta}^{\text{tritium}}(\text{exp})$  to determine  $L_{1A}$ , this program has yet to be carried out.

### 6.3 *Hen* process

In order to gauge the validity of a calculational method used for *Hep*, it is extremely useful to study as a test case the *Hen* process,  ${}^3\text{He} + n \rightarrow {}^4\text{He} + \gamma$ . This is because *Hep* and *Hen* involve similar kinematics and share the characteristic that the contribution of the normally dominant one-body transition operator is highly suppressed owing to the symmetry properties of the wave functions. An EFT\* calculation of *Hen* has been carried out by Song and Park (80), and the calculated cross section,  $\sigma = (60.1 \pm 3.2 \pm 1.0) \mu\text{b}$ , is in reasonable agreement with the experimental values,  $(54 \pm 6) \mu\text{b}$  (40), and  $(55 \pm 3) \mu\text{b}$  (41). This agreement supports the validity of the EFT\* approach in general and the EFT\* calculation of *Hep* in particular, even though there is room for improvements in the  $p$ - ${}^3\text{He}$  continuum wave function used in Reference (80). For the earlier *Hen* calculations based on SNPA, see References (43, 81). It is hoped that there will be further investigations of *Hen* in both SNPA and EFT\*.

## 7 SUMMARY AND OUTLOOKS

As exemplified above, low-energy electroweak processes in light nuclei play important roles in astrophysics, and a recently developed EFT-based formalism, called EFT\* or MEEFT (more effective EFT), can be used profitably to calculate the cross sections of these processes with high precision. We have discussed here *Hep* and a few closely related reactions, but this new method is expected to prove useful for other low-energy electroweak processes as well. The numerical results obtained in EFT\* generally support those obtained in the conventional SNPA, if the strength of the two-body current is controlled by the empirical value of an appropriate observable. It is to be stressed that EFT\* allows us to make

systematic error estimation of the calculated cross sections, a feature that is not readily obtainable in SNPA.

From a formal point of view, one could hope to improve EFT\* by employing nuclear wave functions determined in an EFT formalism itself instead of phenomenological wave functions obtained in SNPA. In regard to observables that do not involve external currents, there has been great progress in building a formally consistent EFT approach applicable to complex nuclei (58, 82). It will be highly informative to apply this type of formalism to electroweak processes and compare the results with those of EFT\*.

### Acknowledgment

The authors gratefully acknowledge useful communications with J.N. Bahcall, M. Rho, M. Fukugita, R. Schiavilla, Y. Suzuki, P. Krastev, F. Myhrer, T. Sato, V. Gudkov, D.-P. Min, S. Ando, S. Nakamura and Y.-H. Song. KK's work is supported in part by National Science Foundation Grant No. PHY-0140214.

### Literature Cited

1. Bahcall JN, Ulrich RK. *Rev. Mod. Phys.* 60:297 (1988)
2. Bahcall JN. *Neutrino Astrophysics* (Cambridge: Cambridge University Press, 1989)
3. Bahcall JN, Pinsonneault MH, Basu S. *Astrophys. J.* 555:990 (2001)
4. Turck-Chièze S, Lopes I. *Astrophys. J.* 408:347 (1993)
5. Bahcall JN, Peña-Garay C. *JHEP* 0311:004 (2003)
6. Davis R, Harmer DS, Hoffman KC. *Phys. Rev. Lett.* 20:1205 (1968); Rowley JK, Cleveland BT, Davis R. *Solar Neutrinos and Neutrino Astronomy*, eds. Cherry ML, Fowler WA, Lande K. (New York: American Institute of Physics) Conference Proceedings No. 126, p. 1
7. Bahcall JN. *Phys. Rev. Lett.* 12:300 (1964)
8. Fukuda Y, *et al.* (Kamiokande Collab.) *Phys. Rev. Lett.* 77:1683 (1996)
9. Fukuda Y, *et al.* (Super-Kamiokande Collab.) *Phys. Rev. Lett.* 81:1158 (1998)

10. Abdurashitov JN, *et al.* (SAGE Collab.) *Phys. Rev. Lett.* 77:4708 (1996)
11. Anselmann P, *et al.* (GALLEX Collab.) *Phys. Lett. B* 342:440 (1995); Hampel W, *et al.* (GALLEX Collab.) *Phys. Lett. B* 388:364 (1996)
12. Ahmad QR, *et al.* (SNO Collab.) *Phys. Rev. Lett.* 87:071301 (2001)
13. Cleveland BT, *et al.* *Astrophys. J.* 496:505 (1998)
14. Fukuda S, *et al.* (Super-Kamiokande Collab.) *Phys. Rev. Lett.* 86:5651 (2001)
15. Gavrin V, *et al.* Presented at VIII Int'l Conf. on Topics in Astroparticle and Underground Physics (TAUP03), Seattle, Sept. 2003; Abdurashitov JN, *et al.* *JETP* 95:181 (2002)
16. Hampel W, *et al.* (GALLEX Collab.) *Phys. Lett. B* 447:127 (1999)
17. Bellotti E. Presented at VIII Int'l Conf. on Topics in Astroparticle and Underground Physics (TAUP03), Seattle, Sept. 2003; Altmann M, *et al.* (GNO Collab.) *Phys. Lett. B* 490:16 (2000)
18. Ahmad QR, *et al.* (SNO Collab.) *Phys. Rev. Lett.* 89:011301 (2002)
19. Ahmad QR, *et al.* (SNO Collab.) *Phys. Rev. Lett.* 89:011302 (2002)
20. Ahmed SN, *et al.* (SNO Collab.) nucl-ex/0309004
21. Bahcall JN. *Phys. Rep.* 333:47 (2000)
22. Pontecorvo B. *Zh. Eksp. Teor. Fiz.* 33:549 (1957) [*Sov. Phys. JETP* 6:429 (1958)]; *Zh. Eksp. Teor. Fiz.* 34:247 (1958) [*Sov. Phys. JETP* 7:172 (1958)]; *Zh. Eksp. Teor. Fiz.* 53:1717 (1967) [*Sov. Phys. JETP* 26:984 (1968)]; *Phys. Lett. B* 26:630 (1968); Gribov V, Pontecorvo B. *Phys. Lett. B* 28:493 (1969)
23. Maki Z, Nakagawa M, Sakata S. *Prog. Theor. Phys.* 28:870 (1962)
24. Mikheyev SP, Smirnov AYu. *Yad. Fiz.* 42:1441 (1985) [*Sov. J. Nucl. Phys.* 42:913 (1985)]; Wolfenstein L. *Phys. Rev. D* 17:2369 (1978)
25. Fukuda Y, *et al.* (Super-Kamiokande Collab.) *Phys. Rev. Lett.* 81:1562 (1998)
26. Eguchi K, *et al.* (KamLAND Collab.) *Phys. Rev. Lett.* 90:021802 (2003)
27. Fukugita M, Yanagida T. *Physics of Neutrinos and Applications to Astrophysics*. Berlin: Springer-Verlag (2003)
28. Bahcall JN. *Phys. Rev. D* 44:1644 (1991)
29. Fukuda Y, *et al.* (Super-Kamiokande Collab.) *Phys. Rev. Lett.* 82:2430 (1999)
30. Fukuda S, *et al.* (Super-Kamiokande Collab.) *Phys. Lett. B* 539:179 (2002)
31. Kuzmin VA. *Phys. Lett.* 17:27 (1965)

32. Escribano R, Frère J-M, Gevaert A, Monderen D. *Phys. Lett. B* 444:397 (1998)
33. Bahcall JN, Krastev PI. *Phys. Lett. B* 436:243 (1998)
34. Marcucci LE, Sciarilla R, Viviani M, Kievsky A, Rosati S, Beacom JF. *Phys. Rev. C* 63:015801 (2001)
35. Salpeter EE. *Phys. Rev.* 88:547 (1952)
36. Wertz C, Brennan JG. *Phys. Rev.* 157:759 (1967)
37. Wertz C, Brennan JG. *Phys. Rev. C* 8:1545 (1973)
38. Tegnér PE, Bargholtz Chr. *Astrophys. J.* 272:311 (1983)
39. Chemtob M, Rho M. *Nucl. Phys. A* 163:1 (1971)
40. Wolfs FLH, Freedman SJ, Nelson JE, Dewey MS, Greene GL. *Phys. Rev. Lett.* 63:2721 (1989)
41. Wervelman R, Abrahams K, Postma H, Booten JGL, Van Hees AGM. *Nucl. Phys. A* 526:265 (1991)
42. Carlson J, Riska DO, Schiavilla R, Wiringa RB. *Phys. Rev. C* 44:619 (1991)
43. Schiavilla R, Wiringa RB, Pandharipande VR, Carlson J. *Phys. Rev. C* 45:2628 (1992)
44. Horowitz CJ. *Phys. Rev. C* 60:022801 (1999)
45. Carlson J, Schiavilla R. *Rev. Mod. Phys.* 70:743 (1998)
46. Riska DO, Brown GE. *Phys. Lett. B* 38:193 (1972); Riska DO. *Phys. Rep.* 181:207 (1989)
47. Ivanov E, Truhlik E. *Nucl. Phys. A* 316:437 (1979); 316:451 (1979); Towner IS. *Phys. Rep.* 155:263 (1987)
48. Weinberg S. *Phys. Lett. B* 251:288 (1990); *Nucl. Phys. B* 363:3 (1991); *Phys. Lett. B* 295:114 (1992)
49. Bernard V, Kaiser N, Meißner U-G. *Int. J. Mod. Phys. E* 4:193 (1995)
50. Brown GE, Rho M. *Phys. Rep.* 363:85 (2002)
51. Georgi H. *Weak Interactions and Modern Particle Physics* (Benjamin, 1984)
52. Weinberg S. *Physica* 96A:327 (1979)
53. Gasser J, Leutwyler H, *Ann. Phys.* 158:142 (1984); Gasser J, Sainio M, Švarc A. *Nucl. Phys. B* 307:779 (1988)
54. Jenkins E, Manohar AV. *Phys. Lett. B* 255:558 (1991)
55. Kaplan DB, Savage MJ, Wise MB. *Nucl. Phys. B* 478:629 (1996); *Phys. Lett. B* 424:390

- (1998); *Nucl. Phys. B* 534:329 (1998)
56. Beane SR, Bedaque PF, Haxton WC, Phillips DR, Savage MJ. In “*At the Frontier of Particle Physics – Handbook of QCD*”, ed. by M. Shifman (World Scientific, Singapore, 2001), Vol. 1, p.133
57. van Kolck U. *Prog. Part. Nucl. Phys.* 43:337 (1999)
58. Bedaque PF, Rupak G, Griebhammer HW, Hammer H-W. *Nucl. Phys. A* 714:589 (2003)
59. Bedaque PF, van Kolck U. *Ann. Rev. Nucl. Part. Sci.* 52:339 (2002)
60. Park T-S, Min D-P, Rho M. *Phys. Rev. Lett.* 74:4153 (1995); *Nucl. Phys. A* 596:515 (1996)
61. Park T-S, Kubodera K, Min D-P, Rho M. *Phys. Rev. C* 58:637 (1998); *Nucl. Phys. A* 646:83 (1999); *Phys. Lett. B* 472:232 (2000); *Nucl. Phys. A (Proc. Suppl.)* 684:101 (2001)
62. Park T-S, Kubodera K, Min D-P, Rho M. *Astrophys. J.* 507:443 (1998)
63. Marcucci LE, Schiavilla R, Viviani M, Kievsky A, Rosati S. *Phys. Rev. Lett.* 84:5959 (2000)
64. Viviani M, Kievsky A, Rosati S. *Few-Body Syst.* 18:25 (1995); Viviani M, Rosati A, Kievsky A. *Phys. Rev. Lett.* 81:1580 (1998)
65. Simpson JJ. *Phys. Rev. C* 35:752 (1987)
66. Park T-S, Marcucci LE, Schiavilla R, Viviani M, Kievsky A, Rosati S, Kubodera K, Min D-P, Rho M. nucl-th/0107012
67. Park T-S, Marcucci LE, Schiavilla R, Viviani M, Kievsky A, Rosati S, Kubodera K, Min D-P, Rho M. *Phys. Rev. C* 67:055206 (2003)
68. Phillips DR, Cohen TD. *Nucl. Phys. A* 668:45 (2000)
69. Bogner S, Kuo TTS, Corragio L. *Nucl. Phys. A* 684:432c (2001); Bogner S, Kuo TTS, Corragio L, Covello A, Itaco N. *Phys. Rev. C* 65:051301 (2002)
70. Adelberger EG, *et al.* *Rev. Mod. Phys.* 70:1265 (1998)
71. Coraddu M, Lissia M, Messorani G, Quarati P. *Physica A* 326:473 (2003)
72. Schiavilla R, *et al.* *Phys. Rev. C* 58:1263 (1998)
73. Park T-S, Marcucci LE, Schiavilla R, Viviani M, Kievsky A, Rosati S, Kubodera K, Min D-P, Rho M. nucl-th/0106025
74. Kong X, Ravendal F. *Nucl. Phys. A* 656:421 (1999); *Nucl. Phys. A* 665:137 (2000); *Phys. Lett. B* 470:1 (1999); Butler M, Chen J-W. *Phys. Lett. B* 520:87 (2001)
75. Butler M, Chen J-W, Vogel P. *Phys. Lett. B* 549:26 (2002); Brown KIT, Butler MN, Guen-

- ther DB. nucl-th/0207008; Balantekin AB, Yüksel H. *J. Phys. G:Nucl. Part. Phys.* 29:665 (2003)
76. Nakamura S, Sato T, Gudkov V, Kubodera K. *Phys. Rev. C* 63:034617 (2001)
77. Nakamura S, Sato T, Ando S, Park T-S, Myhrer F, Gudkov V, Kubodera K. *Nucl. Phys. A* 707:561 (2002); Nakamura S, *et al.*, *Nucl. Phys. A (Proc. Suppl.)* 721:549c (2003)
78. Butler M, Chen J-W. *Nucl. Phys. A* 675:575 (2000); Butler M, Chen J-W, Kong X. *Phys. Rev. C* 63:035501 (2001)
79. Ando S, Song YH, Park T-S, Fearing HW, Kubodera K. *Phys. Lett. B* 555:49 (2003)
80. Song Y-H, Park T-S. nucl-th/0311055
81. Carlson J, Riska DO, Schiavilla R, Wiringa RB. *Phys. Rev. C* 42:830 (1990)
82. Epelbaum E, Glöckle W, Krüger A, Meißner U-G. *Nucl. Phys. A* 645:413 (1999); Epelbaum E, Glöckle W, Meißner U-G. *Nucl. Phys. A* 671:295 (2000); Epelbaum E, Kamada H, Nogga A, Witala H, Glöckle W, Meißner U-G. *Phys. Rev. Lett.* 86:4787 (2001); Epelbaum E, Nogga A, Glöckle W, Kamada H, Meißner U-G, Witala H. *Phys. Rev. C* 66:064001 (2002); *Eur. Phys. J. A* 15:543 (2002)

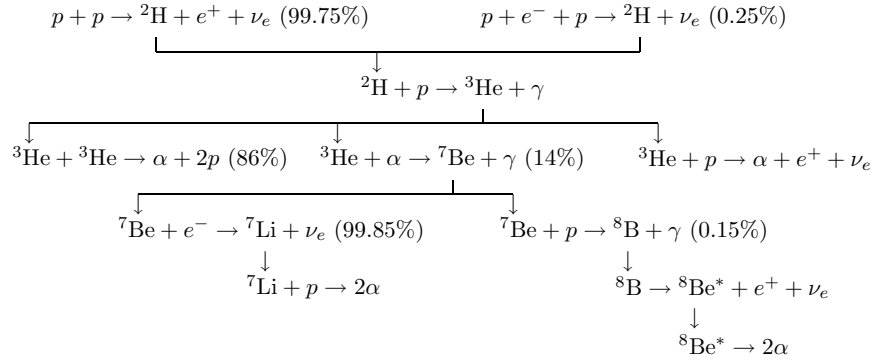


Figure 1: Solar thermonuclear reactions in the  $pp$ -chain and their branching ratios. The  $Hep$  branching ratio is of the order of 0.01% or less.

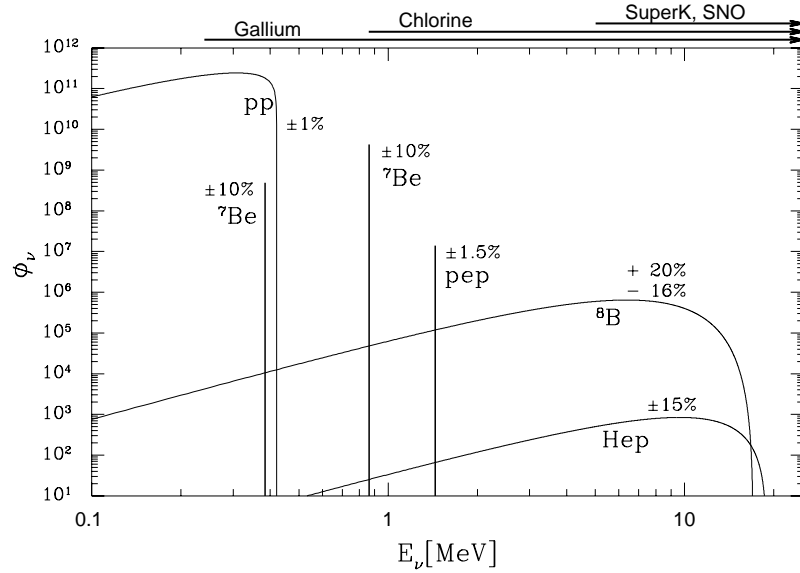


Figure 2: Solar neutrino spectrum  $\phi_\nu$  versus the neutrino energy  $E_\nu$ . The neutrino fluxes from continuum sources are given in units of  $\text{cm}^{-2}\text{s}^{-1}\text{MeV}^{-1}$ , and the line fluxes in units of  $\text{cm}^{-2}\text{s}^{-1}$ . The arrows at the top indicate the ranges of  $E_\nu$  covered by the experiments mentioned in the text.